doi: 10.5028/jatm.v7i4.473

A Novel Integrated Guidance and Control System Design in Formation Flight

Mohammad Sadeghi[1], Alireza Abaspour[1], Seyed Hosein Sadati[1]

ABSTRACT: Bird's formation flight is one of the best types of cooperation in nature. The bird's flight was the motivation of humans for flying. After one century of flight development, bird's formation flight was the motivation of humans for aircraft's formation flight. The closeness of aircrafts in formation flight and the effect of disturbances such as vortex make the formation flight control a challenging issue for control designers. This paper introduces a novel integration between guidance commands and system controller inputs. In recent papers the control system inputs were derived from approximate equations, and this approximation caused maneuver limitation. To tackle this problem, a new method is introduced, which employs proportional-integral-derivative (PID) controller in the integration block. This integrated guidance and control system employs the pure pursuit guidance to determine the unmanned aerial vehicle's acceleration command. A two-loop dynamic inversion technique is used for designing attitude and velocity controller, while the acceleration feedback control is used between the guidance system and attitude controller, which leads to increase in maneuverability of unmanned aerial vehicle's formation flight. The simulation results show that the proposed method can control the UAV's formation with sufficient accuracy in severe maneuvers.

KEYWORDS: Formation flight, Non-linear dynamics, Pure pursuit, Integrated guidance and control.

INTRODUCTION

Unmanned aerial vehicle (UAV) deployments tend to be increasing and their uses seem to be expanding in many aspects. Surveillance, reconnaissance, sampling, and crop-dusting are just some of UAV applications (Watts *et al.* 2012).

In order to guide an UAV in the desired trajectory, the acceleration commands and the angular velocities of the UAV should be calculated by the guidance system. The task of guidance law is to calculate the translational acceleration and angular velocities in order to send them to autonomous flight control system (Lin 1991).

UAV guidance is performed on vertical and lateral-direction. Vertical guidance has to set the vertical distance in the desired point. This system calculates the necessary angle of attack based on vertical distance error and commands them to the longitudinal control system of UAV. The lateral guidance system has to set the UAV in the desired lateral path as well. This system calculates the bank angle commands — in bank to turn (BTT) systems — or side slip angle — in skid to turn (STT) systems — and send them to lateral control system of UAV. Based on the chosen guidance law, the lateral and longitudinal guidance commands can be obtained in two decouple system or in a unique system (Lin 1991; Siouris 2004; CDISS 2003). This paper investigates the leader-follower UAV's formation flight with 3-D pure pursuit guidance method and dynamic inversion flight controller.

In order to enhance the maneuverability of the UAV, dynamic inversion (DI) method is used for designing attitude and velocity controller. DI is a non-linear control technique based on feedback linearization method which eliminates the gain scheduling need by the inversion and cancellation of the

1.Malek Ashtar University of Technology – Aerospace Research Center – Department of Aerospace Engineering – Tehran/Tehran – Iran.

Author for correspondence: Alireza Abaspour | Malek Ashtar University of Technology – Aerospace Research Center – Department of Aerospace Engineering 1774-15875 – Tehran/Tehran – Iran | Email: alireza.abaspour@gmail.com

Received: 02/23/2015 | **Accepted:** 08/26/2015

inherent dynamics, through replacement with a set of user-selected desired dynamics (Reiner *et al.* 1995). Most of the flight controllers designed in this methodology was applied in both longitudinal and lateral/directional axes. This method has been implemented in high-performance aircraft, such as the F-117A (Colgren and Enns 1997) and the F-18HARV (Enns *et al.* 1994), and other modified versions of the F-18 (Adams *et al.* 1994) and the F-16 (Adams and Banda 1993). In this paper a DI technique with two-time scale separation (Sadati *et al.* 2007; Abaspour *et al.* 2013) is applied for the attitude and velocity control of UAV.

Guidance law is the process of generating position commands, and the output of this process is used by flight controller. In contrast with missile guidance, collision avoidance is another important factor in formation of flight guidance. Consequently, the guidance law should hold the head of follower UAV toward the leader UAV, and the velocity control system has to keep the relative desired distance from the target UAV.

The two common guidance laws are proportional navigation (PN) and pure pursuit (PP) guidance law. In this paper PP guidance method is chosen for formation design. The PN method can be also considered as well, but when the PN is used in formation flight, it tends to guide away from the target when the closing velocity is negative (the leader velocity is greater than the follower UAVs) (Yamasaki *et al.* 2009). On the other side, the PP guidance always guides the UAVs independent of the follower and leader velocities. For these reasons, in this paper the pure pursuit guidance law is applied for the formation flight guidance system.

In Giulietti *et al.* (2001) a formation flight control scheme was proposed based on the concept of formation geometry center, which is also known as the formation virtual leader. More complex control laws based on Linear Quadratic Regulator (LQR) and DI approaches have also been proposed in Schumacher and Kumar (2000) and Singh *et al.* 2000. An adaptive approach to vision based on UAV formation control using estimated line of sight (LOS) range was proposed by Sattigeri and Calies (Sattigeri *et al.* 2004). Tahk *et al.* (2005) suggested LOS guidance law for formation flight. The standard synthesized linear quadratic (LQ)-based structure for formation position error control in close formation flight of autonomous aircraft was described in Giulietti *et al.* (2000). The formation-keeping control problem for the three-dimensional autonomous formation flight was addressed in Yang *et al.* (2004) and Min and Tahk (2005).

In order to achieve the desired level of performance and maneuverability, one needs to provide both the required piloting ability (*i.e.* "reflexive skills", typically achieved through a low level feedback control system) and a high-level knowledge of the set of vehicle's achievable behaviors (Stengel 1993).

Stengel (1993) proposes a method for controlling maneuvered formation of autonomous non-holonomic vehicles with the purpose of obtaining a desired target region. This approach was based on tracking of pairs of virtual leaders whose control inputs are obtained in a single optimization process based on model predictive control (MPC) technique.

However, most of the previous results are restricted to two-dimensional formation problem, and full non-linear dynamics of the UAV model is not perfectly considered. Moreover, in previous designs, there was not any guarantee for maintaining formation in lateral acceleration maneuvers. In this paper, instead of routine formulation which was used in previous papers, a new feedback controller is introduced for calculating desired attitude commands from the acceleration commands. Unlike the previous formulation which was used for integrating guidance and control loop, this feedback controller helps to have continual supervision of system integration and, subsequently, a better control performance. As a result, this strategy can help to improve the accuracy of guidance system and formation control. For evaluating the proposed design, two UAV's formation flight, which were modeled by non-linear six degrees-of-freedom (DOF) equations, were used in the simulations. The simulation results show that the proposed method is significantly effective on maneuverability and formation accuracy.

The paper is organized as follows: in "Non-linear UAV Model" section the non-linear mathematical model of aircraft is extracted, whereas DI method is explained in "Dynamic Inversion" section, and the guidance method is described in "Guidance System Design" section. Then in "Numerical Simulations" section we proceed with the numerical simulation, while the conclusions are provided in the final section.

NON-LINEAR UAV MODEL

Accurate flight control system is a must for an UAV; therefore, it is crucial to establish an accurate and practical dynamic model for model based controllers. The plant inputs are delta aileron, delta elevator and delta rudder (δa, δe, δr). The non-linear six DOF equations of motion for an aircraft over a

flat Earth with respect to the body-fixed axis system are depicted in Fig. 1 and are modeled by the following differential equations (Min and Tahk 2005).

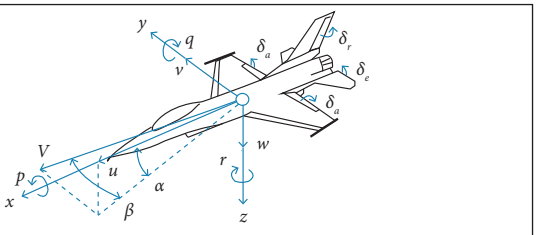

u, *v* and *w*: components of airplane velocity along *x*, *y*, and *z* body axes [m/s].

Figure 1. The aircraft coordinate system.

$$\dot{p} = \frac{I_z l + I_{xz} n}{I_x I_z - I_{xz}^2} r + \frac{I_{xz}(I_x - I_y + I_z) pq}{I_x I_z - I_{xz}^2} + \frac{I[I_z(I_y - I_z) - {I_{xz}}^2]qr}{I_x I_z - I_{xz}^2} \quad (1)$$

$$\dot{q} = \frac{1}{I_y}[m + pr(I_z - I_x) + I_{xz}(r^2 - p^2)] \quad (2)$$

$$\dot{r} = \left[\frac{(I_x - I_y + I_z) I_{xz}}{I_x I_z - I_{xz}^2} r + \frac{I_x(I_x - I_y) + {I_{xz}}^2}{I_x I_z - I_{xz}^2} p\right] q + \frac{I_{xz} l + I_{xx} n}{I_x I_z - I_{xz}^2} \quad (3)$$

$$\dot{\beta} = p \sin\alpha - r\cos\alpha + \frac{1}{M.V}[M.g\sin(\theta - \alpha)\sin\phi] + \frac{1}{M.V}[F_Y \cos\beta - T\sin\beta\cos\alpha] \quad (4)$$

$$\dot{\alpha} = q - (p\cos\alpha + r\sin\alpha)\tan\beta + \frac{1}{M.V\cos\beta}[-L + Mg\cos(\theta - \alpha)\cos\phi] + \frac{1}{M.V\cos\beta}[-T\sin\alpha] \quad (5)$$

$$\dot{\phi} = p + (q\sin\phi + r\cos\phi)\tan\theta \quad (6)$$

$$\dot{\theta} = q\cos\phi - r\sin\phi \quad (7)$$

$$\dot{V} = \frac{1}{M}[-D + F_Y \sin\beta - Mg\sin(\theta - \alpha) + T\cos\beta\cos\alpha] \quad (8)$$

where:

p, q, and r are components of airplane's angular velocity regarding x, y, z body axes [rad/s]; I_x, I_y, and I_z are moments of inertia [kg/m^2] and $I = I_x I_z - I_{xz}^2$; l, m, and n are aerodynamic rolling, pitching, and yawing moment; M is mass [kg]; g is the acceleration due to gravity; V is the velocity; F_x, F_y, and F_z are guidance forces about the body-fixed frame [N]; α is the angle of attack [rad] or [deg]; β is the side slip angle [rad] or [deg]; θ and ϕ are Euler angles [rad] or [deg]; T means thrust [N]; L is lift [N]; ϕ is the rolling angle; $\dot{\theta}$ is the angular velocity regarding to y axis; D is the drag [N].

The drag force, aerodynamic side force (F_y), lift force, and aerodynamic rolling, pitching, and yawing moment, which are used in Eqs. 1–8, can be obtained from the following equations:

$$D = C_{D0} + C_{Da}a + C_{Db}b + C_{Dq}\frac{\bar{cq}}{2V} + C_{Dd_e}d_e \quad (9)$$

$$F_Y = C_{ya}a + C_{yb}b + C_{yp}\frac{bp}{2V} + C_{yr}\frac{br}{2V} + C_{yd_a}d_a + C_{yd_r}d_r \quad (10)$$

$$L = C_{L0} + C_{La}a + C_{Lb}b + C_{Lq}\frac{\bar{cq}}{2V} + C_{Ld_e}d_e \quad (11)$$

$$l = C_{la}a + C_{lb}b + C_{lp}\frac{bp}{2V} + C_{lr}\frac{br}{2V} + C_{ld_a}d_a + C_{ld_r}d_r \quad (12)$$

$$m = C_{m0} + C_{ma}a + C_{mb}b + C_{mq}\frac{\bar{cq}}{2V} + C_{md_e}d_e \quad (13)$$

$$n = C_{na}a + C_{nb}b + C_{np}\frac{bp}{2V} + C_{nr}\frac{br}{2V} + C_{nd_a}d_a + C_{nd_r}d_r \quad (14)$$

where:

C_{D0} is the zero lift drag coefficient; C_D is the drag coefficient; b is the wing span [m]; c is the wing mean aerodynamic chord [m]; C_y is the aerodynamic force coefficient; C_L is the lift coefficient; C_l, C_m and C_n are aerodynamic moment coefficients.

In this paper a WVU YF-22 research airplane is chosen as a test-bed for running the designed aircraft formation flight, whose specification is available on Table 1.

DYNAMIC INVERSION

In this section, we present a feedback linearization technique known as dynamic inversion. DI is a non-linear control design technique based on feedback linearization method and uses a feedback signal to cancel inherent dynamics and simultaneously obtain a desired dynamic response (Reiner *et al.* 1995).

To elaborate the working principle of the non-linear DI (NDI), consider a system of order n with the same number m of inputs u and outputs y and affine in the control inputs. Moreover, the outputs coincide typically to the control variables and are assumed to be physically similar (as an example, attitude angles). This type of system can be mathematically represented by:

$$\begin{aligned} \dot{x} &= f(x) + G(x)u \\ y &= h(x) \end{aligned} \tag{15}$$

where:

f and h are vector fields in R^n and R^m, respectively; $G(x)$ is a $n \times m$ control effectiveness matrix.

This system can be given to any desired dynamics by suitable choice of the control u (Enns *et al.* 1994). For example, the first order dynamics given by Eq. 16 might be chosen.

$$\dot{x} = \dot{x}_d = \omega_c (x_c - x) \tag{16}$$

where:

ω_c is the design parameter chosen by the designer to obtain desire performance; subscript c denotes the commands; subscript d denotes the desired value.

The required control can then be computed by inverting (15):

$$u = G(x)^{-1}(\dot{x}_d - f(x)) \tag{17}$$

Substituting Eq. 17 into Eq. 15, one clearly yields the desired dynamics of Eq. 16. The method can be extended to higher order systems and $G(x)$ is invertible. In flight vehicle control problems, $G(x)$ may be invertible if there

Table 1. WVU YF-22 research aircraft specification and aerodynamic coefficient in cruise flight (Perhinschi *et al.* 2004).

Geometric and inertial			
$c = 0.76$ m	$b = 1.96$ m	$S = 1.37$ m^2	
$I_x = 1.61$ kg/m^2	$I_y = 7.51$ kg/m^2	$I_z = 7.18$ kg/m^2	$I_{xz} = -0.24$ kg/m^2
$M = 20.64$ kg	$F_{Tmax} = 54.62$ N		
Longitudinal aerodynamic derivatives			
$C_{D0} = 0.0085$	$C_{Da} = 0.5079$	$C_{Dq} = 0.0000$	$C_{Dde} = -0.0339$
$C_{L0} = -0.0492$	$C_{La} = 3.258$	$C_{Lq} = -0.0006$	$C_{Lde} = 0.1898$
$C_{m0} = 0.0226$	$C_{ma} = -0.4739$	$C_{mq} = -3.449$	$C_{mde} = -0.3644$
Lateral-directional aerodynamic derivatives			
$C_{Y0} = 0.0156$	$C_{Yb} = 0.2725$	$C_{Yp} = 1.2151$	$C_{Yr} = -1.1618$
$C_{Yda} = 0.1836$	$C_{Ydr} = -0.4592$		
$C_{l0} = -0.0011$	$C_{lb} = -0.0380$	$C_{lp} = -0.2134$	$C_{lr} = 0.1147$
$C_{lda} = -0.0559$	$C_{ldr} = 0.0141$		
$C_{n0} = -0.0006$	$C_n b = 0.0361$	$C_{np} = -0.1513$	$C_{nr} = -0.1958$
$C_{nda} = -0.0358$	$C_{nd} r = -0.0555$		

are sufficient control effectors; however, there will often be conditions where $G(x)$ is nearly singular. This would result in excessively large commands and saturation of control effectors. The near singularity of $G(x)$ is due to the fact that the control moment effectors produce very small forces and thus provide very little direct control of attitude angles. Thus, it is difficult to use dynamic inversion directly for flight vehicle with more or less standard control effectors.

In this paper the problem associated with the invertability of $G(x)$ was overcome by separating the dynamics into slow and fast subsystems in two loops. The fast subsystem corresponds to the body axis angular rates, and the slow subsystem corresponds to the attitude angles. An exact inner loop inversion (fastest) was carried out by using the three control effectors: aileron, elevator, and rudder.

We named these two loops: inner loop, and outer loop controller. The overall diagram of control structure is shown in Fig. 2.

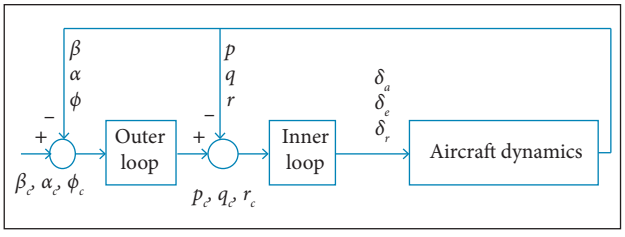

Figure 2. Overall view of designed dynamic inversion controller.

INNER LOOP CONTROLLER

The attitude rates are the fastest states in aircraft model, and in this design they are controlled by the inner loop controller. In two-timescale assumption flight control system, the inner-loop controller is designed to control the fastest states by using the control input u, where the desired values of the fast states are given by the outerloop. Now for using dynamic inversion based on Eqs. 1–3, the fast differential equation can be separated as:

$$\begin{bmatrix}\dot{p}\\ \dot{q}\\ \dot{r}\end{bmatrix}=\begin{bmatrix}f_p(\bar{x})\\ f_q(\bar{x})\\ f_r(\bar{x})\end{bmatrix}+G(x)\begin{bmatrix}\delta_a\\ \delta_e\\ \delta_r\end{bmatrix} \tag{18}$$

while $G(x)$ and $[f_p\, f_q\, f_r]^T$ can be derived from Eqs. 1–3. Considering Eq. 17, the controller of inner loop yields:

$$u=\begin{bmatrix}\delta_a\\ \delta_e\\ \delta_r\end{bmatrix}=G^{-1}(\bar{x})\left(\begin{bmatrix}\dot{p}_d\\ \dot{q}_d\\ \dot{r}_d\end{bmatrix}-\begin{bmatrix}f_p(\bar{x})\\ f_q(\bar{x})\\ f_r(\bar{x})\end{bmatrix}\right) \tag{19}$$

while the desired angular rates are defined by the following equation:

$$\begin{bmatrix}\dot{p}_d\\ \dot{q}_d\\ \dot{r}_d\end{bmatrix}=\begin{bmatrix}\omega_p & 0 & 0\\ 0 & \omega_q & 0\\ 0 & 0 & \omega_r\end{bmatrix}\begin{bmatrix}p_c-p\\ q_c-q\\ r_c-r\end{bmatrix} \tag{20}$$

where:

ω_p, ω_q, and ω_r are inner-loop gain chosen by the designer to obtain desire performance; the subscript c denotes the commands.

OUTER LOOP CONTROLLER

In the outer loop, the controller is designed to control the slow states, and the output of outer loop is used as inner loop commands. The slow states are the attitude angles described in Eqs. 4-6. It is assumed that the fast states track their commanded values instantaneously and the control surface deflection has no effect on the outer loop dynamics.

$$\begin{bmatrix}\dot{\beta}\\ \dot{\alpha}\\ \dot{\phi}\end{bmatrix}=\begin{bmatrix}f_\beta(\bar{x})\\ f_\alpha(\bar{x})\\ f_\phi(\bar{x})\end{bmatrix}+G_{s1}(\bar{x}_{s1})\begin{bmatrix}p\\ q\\ r\end{bmatrix}+G_{s2}(\bar{x}_{s1})\bar{u} \tag{21}$$

Computing the relation between p_c, q_c, and r_c and main control surfaces is difficult, so the small term $G_{s2}(\bar{x}_{s1})$ is neglected. Considering Eq. 21, the controller of outer loop yields:

$$\begin{bmatrix}\dot{\beta}\\ \dot{\alpha}\\ \dot{\phi}\end{bmatrix}\approx\begin{bmatrix}f_\beta(\bar{x})\\ f_\alpha(\bar{x})\\ f_\phi(\bar{x})\end{bmatrix}+G_{s1}(\bar{x}_{s1})\begin{bmatrix}p\\ q\\ r\end{bmatrix} \tag{22}$$

while the desired angular variables' derivatives defined by the following equation are:

$$\begin{bmatrix}\dot{\beta}_d\\ \dot{\alpha}_d\\ \dot{\phi}_d\end{bmatrix}=\begin{bmatrix}\omega_\beta & 0 & 0\\ 0 & \omega_\alpha & 0\\ 0 & 0 & \omega_\phi\end{bmatrix}\begin{bmatrix}\beta_c-\beta\\ \alpha_c-\alpha\\ \phi_c-\phi\end{bmatrix} \tag{23}$$

where:

ω_β, ω_ϕ, and ω_α are outer loop control gains, which are chosen by the designer to obtain desired performance; β_c, α_c, and ϕ_c are guidance system commands.

By using Eq. 22, the output of outer loop is derived as the following equation:

$$\begin{bmatrix} p_c \\ q_c \\ r_c \end{bmatrix} = G^{-1}{}_{s1}(\bar{x}_{s1}) \left(\begin{bmatrix} \dot{\beta}_d \\ \dot{\alpha}_d \\ \dot{\phi}_d \end{bmatrix} - \begin{bmatrix} f_\beta(\bar{x}) \\ f_\alpha(\bar{x}) \\ f_\phi(\bar{x}) \end{bmatrix} \right)$$

VELOCITY CONTROLLER

In this paper the guidance method, which is used for the trajectory tracking, is pure pursuit. Due to pure pursuit nature, this guidance system heads to a target point only, and does not care for the velocity control along the velocity vector. For this reason, a velocity control system is necessary to keep a desired distance from the given trajectory. The velocity controller is also designed based on the dynamic inversion approach, and the aircraft dynamics is considered as well.

According to the aircraft closeness in formation flight, velocity control has an important role for collision avoidance. The designed velocity controller, which is used in this paper, has two control loops. One of them is velocity and the other one is relative distance. This loop separation is based on time scale separation assumption. This conception is clearly shown in Fig. 3 with block diagram.

As it can be seen in Fig. 3, R_d and V_d are desired distance and velocity, respectively. The look up table block, which is drawn on Table 2, calculates V_d according to error from the reference (e_R).

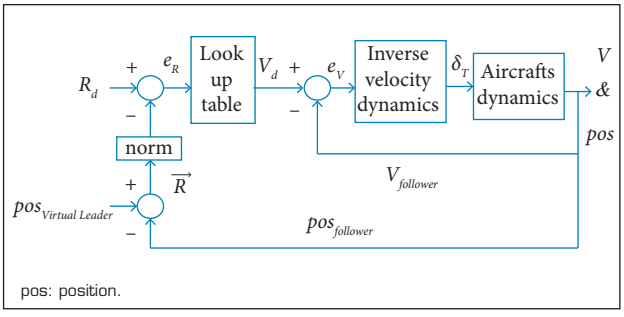

Figure 3. Velocity controller's structure.

Table 2. Velocity controller look up table.

e_R(m)	V_d(m/s)
< −300	V_{max}
−5	$V_{virtual\ leader}$
0	V_{min}

The DI velocity controller is designed based on Eq. 8. By solving this equation based on thrust force (F_T) and replacing U_a instead of $\dot{V}$, and desired thrust force (F_{Td}) instead of F_T, the thrust command can be calculated. By dividing F_{Td} with maximum thrust (F_{Tmax}), δ_T (thrust control input) can be obtained by following equation:

$$\delta_T = F_{Td}/F_{Tmax} = \{m.(U_a) - m.g.(-\sin\theta.\cos\alpha.\cos\beta + \cos\theta.\sin\varphi.\sin\alpha.\cos\beta) + D.\cos\beta\}/\{(\cos\alpha.\cos\beta)^* F_{Tmax}\} \quad (25)$$

where:

U_a is the control input and can be obtained as follows:

$$U_a = K_V \dot{e}_v \quad (26)$$

where:

K_v is a control gain, and in this paper it is equaled to 1; e_v is the relative velocity error.

GUIDANCE SYSTEM DESIGN

The guidance system's task in formation flight is to direct the UAV in a path, which minimizes the leader and follower aircraft's distance. In this system the needed acceleration for approaching to the leader aircraft is calculated, and its output is used as the control system input of the UAV (Lin 1991). The guidance system guides the UAV in two directions: vertical and horizontal. The vertical guidance calculates the vertical acceleration commands and the angle of attack, while the horizontal guidance is used to locate the aircraft in desired lateral path. This system does this task by comparing the current position in horizontal plane with the desired one; therefore, the system provides the needed acceleration to keep the aircraft with desired path. In other words, in bank to turn (BTT) systems, the horizontal guidance calculates the bank angle command. This command will be used in lateral position control (Siouris 2004; CDISS 2003).

Pure pursuit guidance law and proportional navigation guidance law are the most conventional methods which are used for guiding goals (Naeem *et al.* 2003). In this paper pure pursuit law is chosen for its simplicity and its accuracy in formation flight (Enomoto *et al.* 2010).

PURE PURSUIT

Pure pursuit is one of the most conventional methods in guidance laws. In this law the follower has to keep its line of

sight in line of target movement. In other words, the direction of the velocity vector has to be in line with the target site (Naeem *et al.* 2003).

Just like missile system, we can use the pure pursuit guidance law in formation flight. If we denote the line of sight vector between the follower aircraft and virtual leader (the desired point that follower track it) with $\vec{R}$, and the follower aircraft speed vector with $\vec{V}_f$ to coincide the follower speed vector with line of sight, the following equation should be established:

$$\vec{V}_f \times \vec{R} = 0 \tag{27}$$

Figure 4 shows the relation between R and V_f vectors, where d_{xref} denotes the distance between leader and virtual leader in longitudinal axis; d_{yref} denotes the distance in lateral axis; d_{zref} denotes the distance in vertical axis. The acceleration commands for moving the aircraft toward the virtual leader is obtained from the following equation (Shneydor 1998; Yamasaki *et al.* 2008):

$$\vec{A}_f = \frac{N(\vec{V}_f \times \vec{R}) \times \vec{V}_f}{norm(\vec{V}_f).norm(\vec{R})} \tag{28}$$

Finally, by using Newton's second law and considering the weight, the needed guiding force is obtained as follows:

$$\vec{F}_f = M\frac{N(\vec{V}_f \times \vec{R}) \times \vec{V}_f}{norm(\vec{V}_f).norm(\vec{R})} + M\vec{g} \tag{29}$$

where:

$\vec{g}$ is the Earth's gravity vector; M is the airplane mass; N is the navigational coefficient. In this equation the navigational coefficient is usually chosen between 0.5 to 3, and choosing a larger coefficient increases the amplitude of maximum guidance acceleration commands, especially in initial time of the formation.

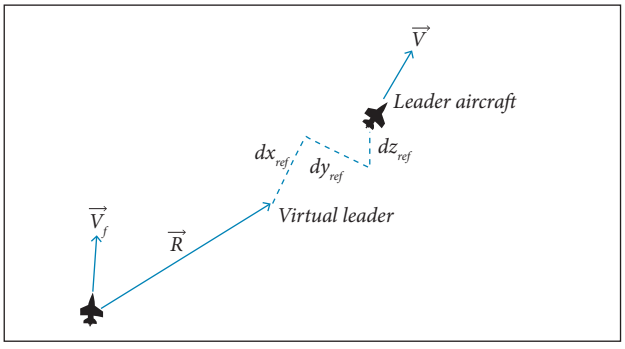

Figure 4. Pure pursuit tracking (Shneydor 1998).

TRANSFORMATION OF GUIDANCE ACCELERATIONS INTO INNER LOOP CONTROLLER COMMANDS

The acceleration commands are achieved by guidance law, and the direction and magnitude of the force vector can be generated by the UAV's slow dynamic states. In this paper, slow dynamic states are the angle of attack, side slip angle, and bank angle.

The system, which is used in this paper, is BTT. Therefore, the desired side slip angle is zero. As a result, in order to obtain and maintain the formation, the angle of attack and bank angle should be obtained by the guidance commands. According to the fact that guidance commands are in inertial coordination, for making an integrated guidance and control, they should rotate from inertial axis to body axis. For this reason, the rotational matrix is used as follows (Fossen 2011):

$$T_B^{NED} = \begin{bmatrix} c\psi c\theta & -s\psi.c\phi + c\psi.s\theta.s\phi & s\psi.s\phi + c\psi.c\phi.s\theta \\ s\psi.c\theta & c\psi.c\phi + s\phi.s\theta.s\psi & -c\psi.s\phi + s\theta.s\psi.c\phi \\ -s\theta & c\theta.s\phi & c\theta.c\phi \end{bmatrix} \tag{30}$$

where:

T^{B}_{NED} is the rotation matrix from the North-East-Down (NED) axes to the body axes; c denotes cosine; s denotes sine; Ψ is an Euler angle.

The angle of attack (α) and the bank angle (ϕ) generate the longitudinal and lateral acceleration in airplane guidance system, respectively. Therefore, to reduce the difference between the acceleration commands from body coordinate ($Nz_{Bguidance}/Ny_{Bguidance}$) and the actual acceleration of airplane in body coordination ($Nz_{Baircraft}/Ny_{Baircraft}$), the control inputs of airplane attitude (α_c, ϕ_c) should be calculated via acceleration error (E_{NzB}/E_{NyB}). This operation can be done through the control law (F) which is described as:

$$\alpha_C = F(E_{Nz_B})$$
$$E_{Nz_B} = Nz_{Bguidance} - Nz_{Baircraft} \tag{31}$$

$$\phi_C = F(E_{Ny_B})$$
$$E_{Ny_B} = Ny_{Bguidance} - Ny_{Baircraft} \tag{32}$$

where:

F is the controller, which can be classic, adaptive or DI. As it can be seen in Fig. 5, in this paper PID controller is used for this purpose. In Fig. 5, N_{zc_body} and N_{yc_body} are the vertical and horizontal body coordination systems, respectively. Also, $N_{z\_Res\_body}$ and $N_{y\_Res\_body}$ are the vertical and horizontal acceleration responses, respectively.

The last step in formation flight control design is integrating the control and guidance systems. The overall view of the designed system can be seen in Fig. 6. As it can be seen in this figure, to control and guide the follower UAV, only the virtual leader position is needed, which is easily available. The virtual leader position is subtracted from follower position, and the vector of R is obtained. This vector and the velocity vector are sent to guidance block, in which the needed acceleration is calculated for approaching to the virtual leader. Then, this acceleration is converted to angle of attack and bank angle by guidance-control integration block. Finally, the produced attitude commands are sent to outer loop controller for obtaining the desired position. In addition, the velocity controller has to obtain the desired distance between follower and leader, at the same time.

NUMERICAL SIMULATIONS

In this paper a novel integrated guidance-control system is designed for UAV formation purposes. In this section numerical simulation was carried out for evaluation of the introduced design. Several simulations using the WVU YF-22 model have been conducted, as a follower UAV. Table 3 gives the initial condition and parameter settings of these simulations. The following assumptions were made to simplify the problem and to demonstrate the total system performance:

The UAV model is available and aerodynamic uncertainties are negligible.

The target UAV's direction, distance and relative velocity information are available.

In order to evaluate the proposed design, a scenario is defined for formation flight, whose specification is available on Table 3. A virtual leader is assumed, which has a small distance in relation to the actual leader. This assumption is based on the collision avoidance of leader and follower.

The navigation constant is chosen as 1 and the integrator controller gains are set according to Table 4.

As it can be seen in Fig. 7, the follower aircraft tracked the virtual aircraft accurately. Despite the fact that a significant difference among UAV's initial conditions was considered and the maneuver was complicated, the follower successfully tracked the virtual leader. Moreover, the follower has not any collision with the leader.

For a better formation analysis, the (x-y) and (x-z) plots of the formation are depicted on Figs. 8 and 9, respectively.

Figures 8 and 9 show that the designed system can track the desired trajectory accurately. The vertical command, which is produced by guidance system, is depicted on Fig. 10, in which the tracking of this command is depicted as well.

Figure 10 shows that the vertical acceleration error is successfully compensated by the angle of attack. Also, the tracking of the lateral acceleration, which is produced by guidance loop, is shown in Fig. 11, in which it can be clearly seen that the lateral acceleration error is successfully compensated by bank angle.

The control deflection is another important factor for the control designers. The domain of their changes should not be larger than the actuator domains. Also, due to mechanical consideration, it is better to not have an oscillatory change in control deflections. Figure 12 shows the control deflection of the follower aircraft in the desired trajectory. As it can be seen, the aircraft has a desirable control deflection.

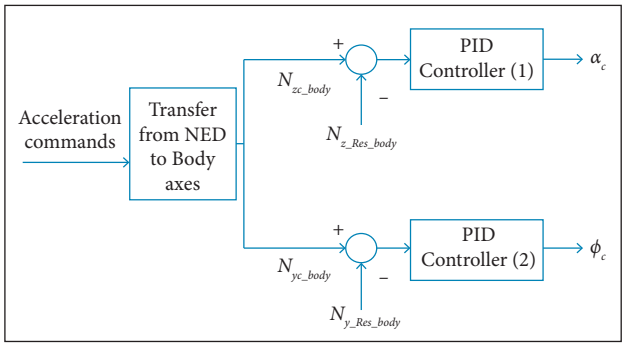

Figure 5. Guidance and control integrator.

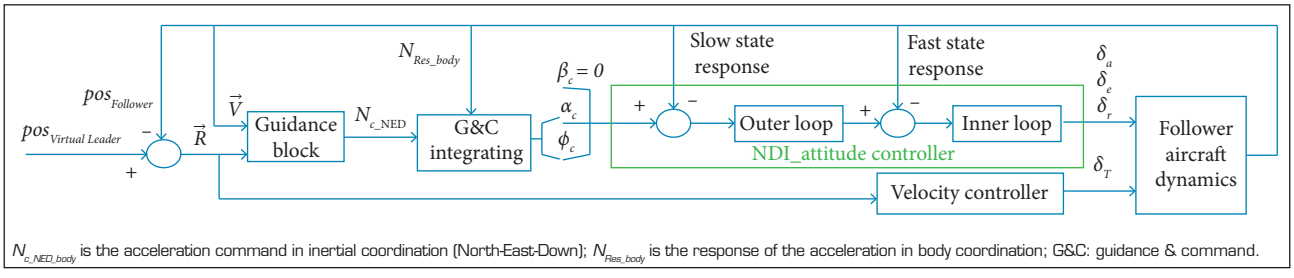

Figure 6. The integrated guidance and control system diagram.

Table 3. Formation scenario.

	Leader's position	Virtual leader's position
Longitudinal axis	$X_l = 110 + 150t$	$X_{vl} = 100 + 150t$
Lateral axis	$Y_l = 110 + 40\sin(0.1t) + 2t$	$Y_{vl} = 100 + 40\sin(0.1t) + 2t$
Vertical axis	$H_l = 1100 + 40\cos(0.1t) + 2t$	$H_{vl} = 1100 + 40\cos(0.1t) + 2t$

Table 4. The integrator controller specification.

Gain	Lateral	Longitudinal
Derivative gain	–0.01	0
Proportional gain	–0.08	0.003
Integrative gain	0	0.01

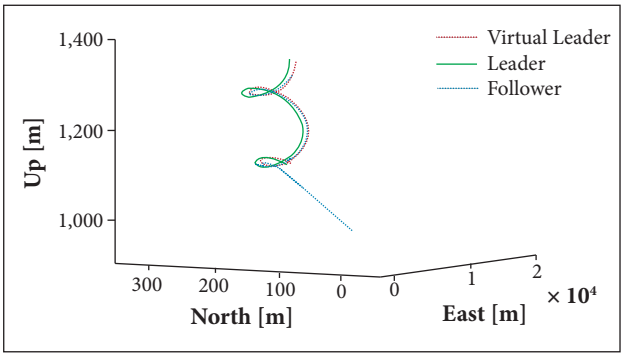

Figure 7. The three-dimensional view of leader, virtual leader and the follower.

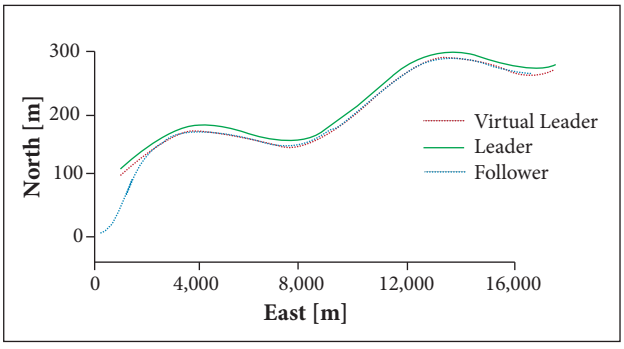

Figure 8. The (*x-y*) view of leader, virtual leader and the follower.

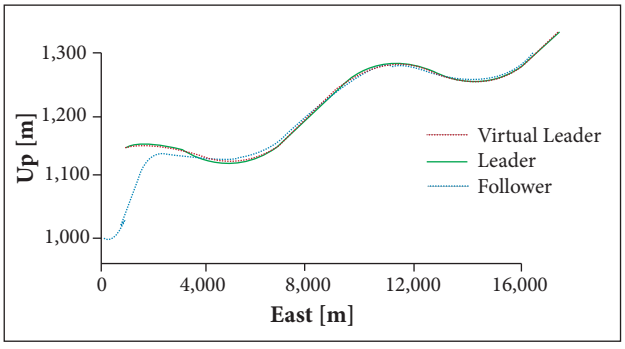

Figure 9. The (*x-z*) view of leader, virtual leader and the follower.

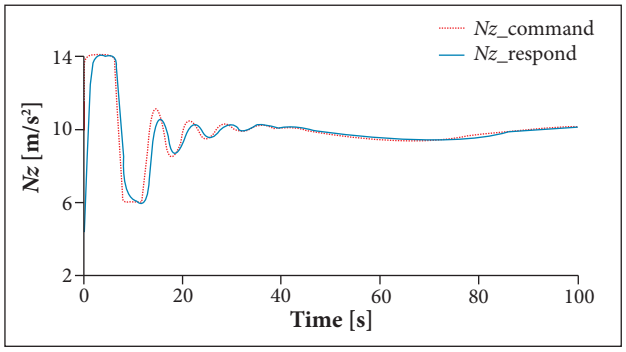

Figure 10. The longitudinal acceleration produced by guidance loop ($N_{z\text{-command}}$) and the follower tracking of it ($N_{z\text{-output}}$).

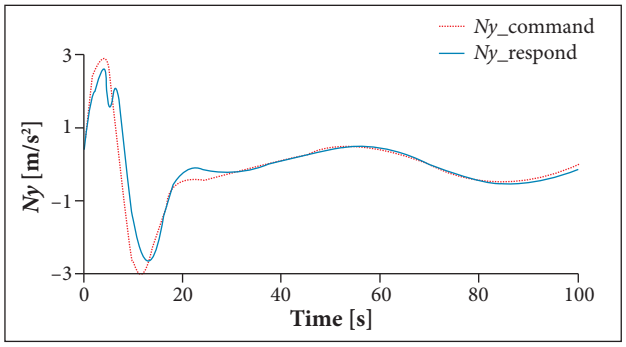

Figure 11. The lateral acceleration produced by guidance loop ($N_{y\text{-command}}$) and the follower tracking of it ($N_{y\text{-response}}$).

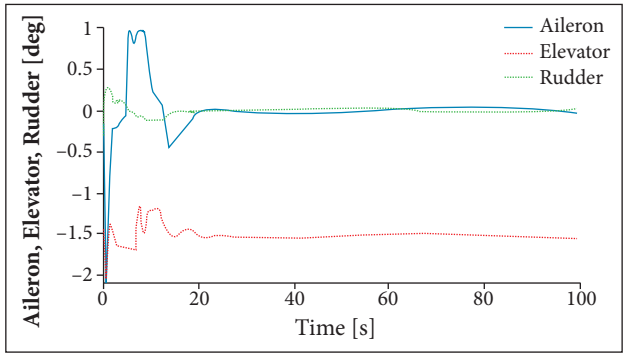

Figure 12. Control deflection of aileron, elevator and rudder.

Figure 13 deals with the DI controller accuracy. This controller is designed in two loops: inner loop and the outer loop controller. As it can be seen in this figure, the commanded attitudes and rates are tracked precisely.

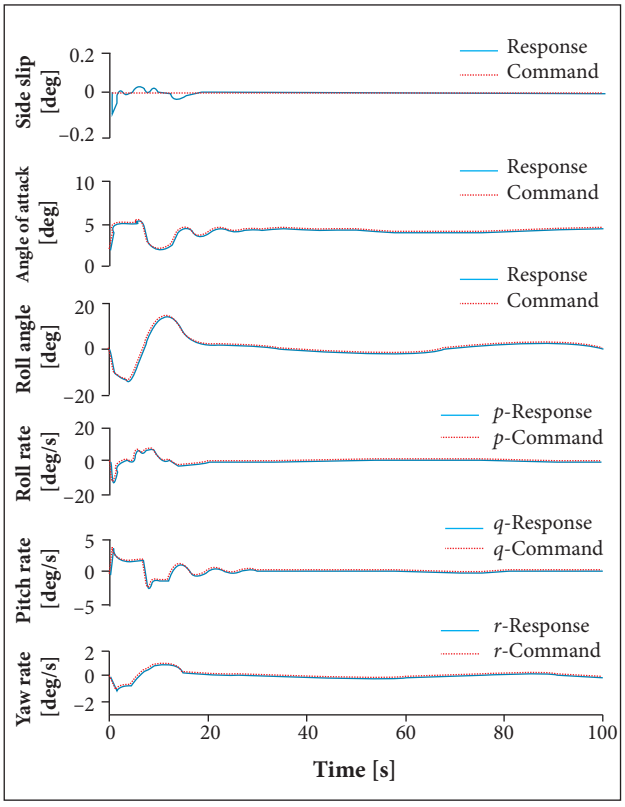

Figure 13. The DI control performance in tracking-commanded attitudes and rates.

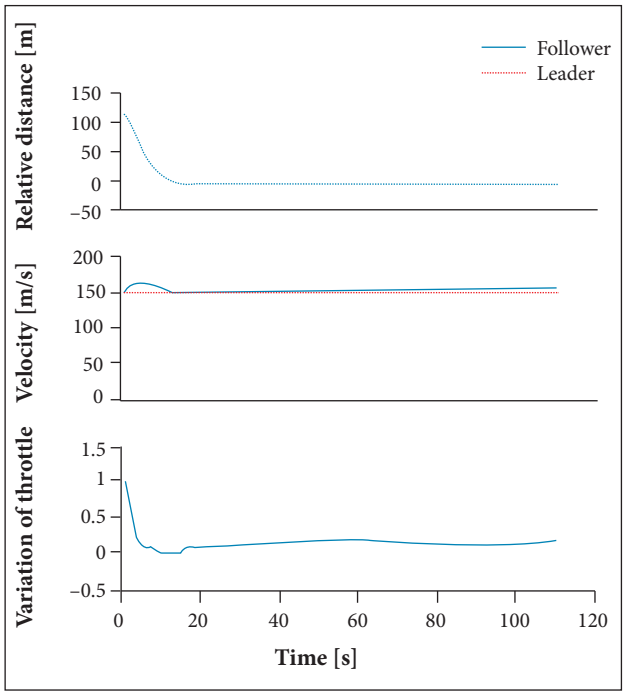

Figure 14. The designed control performance in velocity, relative-distance and throttle variation.

The velocity control is another important factor in formation design. Thus, the ability of the proposed controller in tracking the desired speed and the desired distance with the leader is depicted on Fig. 14. The throttle which is the control input for velocity control is plotted in this figure, which demonstrates that the designed velocity controller has desirable performance.

CONCLUSION

In this paper a new integration method for integrating the control and guidance systems of an aircraft is introduced. Then, this method is used to establish aircraft formation flight. The novelty of this method is using PID controller in integration block, instead of common formulation, which has been done in previous papers. This PID controller helped to have a better feedback from the control and guidance integration, and subsequently a better formation flight. The dynamic specification of WVU YF-22 research aircraft is used to demonstrate the ability of this method. Moreover, non-linear dynamic inversion is used to control the airplane attitude and its velocity. Finally, numerical simulation is done via MATLAB Simulink software. The simulation results show that the proposed method can successfully control the formation flight in several maneuvers. From these results, it can be concluded that the introduced integration method can be used in order to integrate guidance and control precisely. Consequently, an accurate formation flight is obtained by using the introduced method.

REFERENCES

Abaspour A, Sadeghi M, Sadati SH (2013) Using Fuzzy Logic In Dynamic Inversion Flight Controller With Considering Uncertainties. Proceedings of the 13th Iranian Conference on Fuzzy Systems; Ghazvin, Iran.

Adams RJ, Banda SV (1993) Robust flight control design using dynamics inversion and structured singular value synthesis. IEEE T Contr Syst T 1(2):80-92. doi: 10.1109/87.238401

Adams RJ, Buffington JM, Banda SV (1994) Design of nonlinear control laws for high-angle-of-attack flight. J Guidance Control Dynam 17(4):737-746. doi: 10.2514/3.21262

CDiSS (2003) Cruise missiles key technologies: an overview. Lancaster, UK: Center for Defence and International Security Studies.

Colgren R, Enns D (1997) Dynamic inversion applied to the F-117A.

Proceedings of the AIAA Modeling and Simulation Technologies Conference, AIAA; Reston, USA.

Enns D, Bugajski D, Hendrick R, Stein G (1994) Dynamic inversion: an evolving methodology for flight control design. Int J Control 59(1):71-91. doi: 10.1080/00207179408923070

Enomoto K, Yamasaki T, Takano H, Bab Y (2010) A study on a velocity control system design using the dynamic inversion method. Proceedings of the AIAA Guidance, Navigation, and Control Conference; Toronto, Canada.

Giulietti F, Pollini L, Innocenti M (2000) Autonomous formation flight. IEEE Contr Syst Mag 20(6):34-44.

Giulietti F, Pollini L, Innocenti M (2001) Formation flight control: a behavioral approach. Proceedings of the 2001 AIAA GNC Conference; Montreal, Canada.

Lin CF (1991) Modern navigation: guidance and control processing. Englewood Cliffs, NJ: Prentice Hall.

Min BM, Tahk MJ (2005) Three-dimensional Guidance Law for Formation Flight of UAV. Proceedings of the International Conference on Control, Automation and Systems; Gyeonggi-Do, South Korea.

Naeem W, Sutton R, Ahmad SM, Burns RS (2003) A review of guidance laws applicable to unmanned underwater vehicles. J Nav 56(1):15-29. doi: 10.1017/S0373463302002138

Perhinschi MG, Napolitano MR, Campa G, Seanor B, Gururajan S (2004) Design of intelligent flight control laws for the WVU YF-22 model aircraft. Proceedings of the AIAA 1st Intelligent Systems Technical Conference; Chicago, USA.

Reiner J, Balas GJ, Garrard WL (1995) Robust dynamic inversion for control of highly maneuverable aircraft. J Guidance Control Dynam 18(1):18-24. doi: 10.2514/3.56651

Sadati SH, Sabzeh Parvar M, Menhaj MB, Bahrami M (2007) Backstepping controller design using neural networks for a fighter aircraft. Eur J Control 13(5):516-526. doi: 10.3166/ejc.13.516-526

Sattigeri R, Calise AJ, Evers JH (2004) An adaptive vision-based approach to decentralized formation control. Proceedings of the AIAA Guidance, Navigation, and Control Conference; Providence, USA.

Schumacher CJ, Kumar R (2000) Adaptive control of UAVs in close coupled formation flight. Proceedings of the 2000 American Control Conference; Chicago, USA.

Shneydor N (1998) Missile guidance and pursuit: kinematics, dynamics and control. Woodgate, UK: Horwood Publishing.

Singh SN, Pachter M, Chandler P, Banda S, Rasmussen S, Schumacher CJ (2000) Input-output invertibility and sliding mode control for close formation flying of multiple UAVs. Proceedings of the 2000 AIAA GNC Conference; Denver, USA.

Siouris GM (2004) Missile guidance and control systems. New York: Springer.

Stengel RF (1993) Towards intelligent flight control. IEEE Trans Syst Man Cybern 23(6):1699-1717. doi: 10.1109/21.257764

Tahk MJ, Park CS, Ryoo CK (2005) Line-of-sight guidance laws for formation flight. J Guidance Control Dynam 28(4):708-716. doi: 10.2514/1.9605

Fossen TI (2011) Mathematical models for control of aircraft and satellites. Trondheim: Norwegian University of Science and Technology.

Watts AC, Ambrosia VG, Hinkley EA (2012) Unmanned aircraft systems in remote sensing and scientific research: classification and considerations of use. Remote Sens 4(6):1671-1692. doi: 10.3390/rs4061671

Yamasaki T, Takano H, Baba Y (2008) Robust path-following for UAV using pure pursuit guidance. National Defense Academy, Japan.

Yamasaki T, Enomoto K, Takano H, Baba Y (2009) Advanced pure pursuit guidance via sliding mode approach for chase UAV. Proceedings of the AIAA Guidance, Navigation, and Control Conference; Chicago, USA.

Yang E, Masuko Y, Mita T (2004) Dual-controller approach to three-dimensional autonomous formation control. J Guidance Control Dynam 27(3):336-346. doi: 10.2514/1.1562